Steric and Electronic Effects, Enantiospecificity, and Reactive Orientation in DNA Binding/Cleaving by Substituted Derivatives of [SalenMn^{III}]$^+$

Dennis J. Gravert and John H. Griffin*

Department of Chemistry, Stanford University, Stanford, California 94305-5080

Received February 22, 1996[⊗]

Twenty-six derivatives of [SalenMn^{III}]$^+$ (**1**) bearing halogen, nitro, amino, ether, alkyl, or aryl substituents on the aromatic rings and/or at the imine positions or containing 1,3-propylene-, 1,2-phenylene-, 1,2-cyclohexane-, or 1,2-diphenylethylenediamine in place of ethylenediamine as the bridging moiety have been synthesized. The DNA binding/cleaving properties of these complexes in the presence of terminal oxidants have been examined using DNA affinity cleaving techniques. Active derivatives produced DNA cleavage from the minor groove at sites containing multiple contiguous A:T base pairs. For aryl-substituted derivatives, DNA cleavage efficiency was found to vary with both the identity and position of attachment of substituents. The precise patterns of cleavage at A:T target sites varied with the position of attachment of substituents, but not with the identity of the substituents. The results suggest that substituents alter specificity through both steric and electronic effects. The 3,3′-difluoro and -dichloro derivatives produced cleavage patterns that match those of the parent complex, suggesting that the activated form of **1** produces cleavage from an orientation in which the concave edge of the complex faces away from the floor of the DNA minor groove. Bridge modifications yield complexes with reduced DNA cleaving activity relative to **1**. DNA cleaving efficiency was found to vary with both the structure and stereochemistry of the bridge. Cleavage efficiency for the complex derived from (*R,R*)-cyclohexanediamine was 5 times greater than that for the (*S,S*) enantiomer. Cleavage patterns produced by the enantiomeric complexes at A:T rich target sites were different, demonstrating enantiospecific recognition and cleavage of right-handed double-helical DNA.

Introduction

We recently reported that [SalenMn^{III}]$^+$ (**1**, Salen = *N,N*′-ethylenebis(salicylideneaminato)) mediates the cleavage of right-handed double-helical DNA in the presence of terminal oxidants.[1] The combination of **1** and oxidant produces single-strand cleavage as well as double-strand cleavage which derives from independent, proximal nicks on opposite DNA strands. Cleavage is effected selectively from the DNA minor groove in segments rich in A:T base pairs and is consistent with a mechanism involving deoxyribose C−H activation by an oxidatively activated intermediate such as [SalenMn^{V}O]$^+$.[2,3] Complex **1** produces cleavage in regions of DNA that are targeted by netropsin-like affinity cleaving agents and neocarzinostatin but only weakly cleaved by bleomycin:Fe and methidiumpropyl−EDTA:Fe.[4] These findings, when coupled with the knowledge that substituents modulate the properties of **1** as a catalyst for hydrocarbon oxidation[2,5] and that changes in ligand structure and stereochemistry can alter the DNA binding/cleaving properties of metalloporphyrins,[6] octahedral cobalt and rhodium complexes,[7] bis(1,10-phenanthroline):copper complexes,[8] and macrocycle:nickel complexes,[9] have prompted us to consider and probe the effects that structural modifications have on the DNA binding/cleaving properties of **1**.

In this paper, we report the synthesis of 26 derivatives of the crescent-shaped, cationic parent complex bearing symmetrical substitutions on the aryl rings, at the imine positions, or on the bridge and the analysis of their DNA binding/cleaving properties. We find that the addition of substituents to **1** has large effects on DNA binding/cleaving efficiency and induces changes in cleavage patterns within A:T rich target sites. The results have a number of implications for the role(s) of substituent effects in DNA recognition and cleavage by [SalenMn^{III}]$^+$

* To whom correspondence should be addressed: phone (415) 723-3625; fax (415) 725-0259; email jgriffin@leland.stanford.edu.

⊗ Abstract published in *Advance ACS Abstracts,* July 15, 1996.

(1) Gravert, D. J.; Griffin, J. H. *J. Org. Chem.* **1993**, *58*, 820−822.
(2) Srinivasan, K.; Michaud, P.; Kochi, J. K. *J. Am. Chem. Soc.* **1986**, *108*, 2309−2320.
(3) In preliminary studies of the cleavage mechanism, we have determined that the combination of [SalenMn^{III}]$^+$ and oxidant produces direct DNA strand breaks and base-labile lesions through processes that do not involve dioxygen. DNA cleavage releases free, unmodified nucleotide bases. The DNA termini produced consist of 3′ phosphate groups as well as 5′ phosphate and 5′ nonphosphate, nonhydroxyl groups that are converted to phosphates by base treatment. Addition of substituents to [SalenMn^{III}]$^+$ does not substantially alter the observed reaction pathways.
(4) Griffin, J. H. *Bioorg. Med. Chem. Lett.* **1995**, *5*, 73−76.
(5) Jacobsen, E. N.; Zhang, W.; Güler, M. L. *J. Am. Chem. Soc.* **1991**, *113*, 6703−6704.
(6) (a) Bromley, S. D.; Ward, B. W.; Dabrowiak, J. C. *Nucleic Acids Res.* **1986**, *14*, 9133−9148. (b) Raner, G.; Ward, B; Dabrowiak, J. C. *J. Coord. Chem.* **1988**, *19*, 17. (c) Sehlstedt, U.; Kim, S. K.; Carter, P.; Goodisman, J.; Vollano, J. F.; Nordén, B.; Dabrowiak, J. C. *Biochemistry* **1994**, *33*, 417−426.
(7) (a) Raphael, A. L.; Barton, J. K. *J. Am. Chem. Soc.* **1984**, *106*, 2466−2468. (b) Raphael, A. L.; Barton, J. K. *Proc. Natl. Acad. Sci. U.S.A.* **1985**, *82*, 6460−6464. (c) Pyle, A. M.; Long, E. C.; Barton, J. K. *J. Am. Chem. Soc.* **1989**, *111*, 4520−4522. (d) Pyle, A. M.; Morii, T.; Barton, J. K. *J. Am. Chem. Soc.* **1990**, *112*, 9432−9434. (e) Sitlani, A.; Long, E. C.; Pyle, A. M.; Barton, J. K. *J. Am. Chem. Soc.* **1992**, *114*, 2303−2312. (f) Krotz, A. H.; Kuo, L. Y.; Shields, T. P.; Barton, J. K. *J. Am. Chem. Soc.* **1993**, *115*, 3877−3882. (g) Krotz, A. H.; Hudson, B. P.; Barton, J. K. *J. Am. Chem. Soc.* **1993**, *115*, 12577−12578. (h) Sitlani, A.; Dupureur, C. M.; Barton, J. K. *J. Am. Chem. Soc.* **1993**, *115*, 12589−12590. (i) Campisi, D.; Morii, T.; Barton, J. K. *Biochemistry* **1994**, *33*, 4130−4139. (j) Sitlani, A.; Barton, J. K. *Biochemistry* **1994**, *33*, 12100−12108.
(8) (a) Sigman, D. S. *Acc. Chem. Res.* **1986**, *19*, 180−186. (b) Thederahn, T. B.; Kuwabara, M. D.; Larsen, T. A.; Sigman, D. S. *J. Am. Chem. Soc.* **1989**, *111*, 4941−4946.
(9) (a) Muller, J. G.; Chen, X.; Dadiz, A. C.; Rokita, S. E.; Burrows, C. J. *J. Am. Chem. Soc.* **1992**, *114*, 6407−6411. (b) Burrows, C. J.; Rokita, S. E. *Acc. Chem. Res.* **1994**, *27*, 295−301.

S0020-1669(96)00196-6 CCC: $12.00

Table 1. Ring- and Imine-Substituted $[SalenMn^{III}]^+$ Derivatives

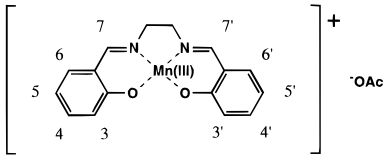

1	Unsub.	**4**	3,3'-Cl_2	**9**	5,5'-Br_2	**14**	4,4'-$(Et_2N)_2$
2	3,3'-F_2	**5**	4,4'-Cl_2	**10**	5,5'-$(NO_2)_2$	**15**	7,7'-Ph_2
3	5,5'-F_2	**6**	5,5'-Cl_2	**11**	3,3'-$(OCH_3)_2$	**16**	7,7'-$(CH_3)_2$
		7	6,6'-Cl_2	**12**	4,4'-$(OCH_3)_2$	**17**	4,4'-$(OCH_3)_2$-7,7'-$(CH_3)_2$
		8	3,3',5,5'-Cl_4	**13**	5,5'-$(OCH_3)_2$		

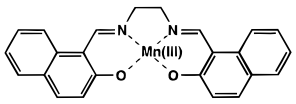

18 [NaphenMn(III)]$^+$

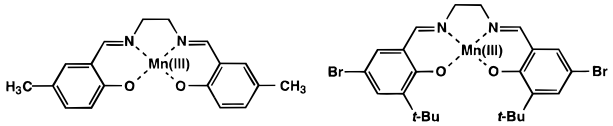

19 5,5'-$(CH_3)_2$ **20** 5,5'-Br_2-3,3'-*t*-Bu_2

derivatives. Most significantly, our data (1) provide evidence that both steric and electronic effects alter the DNA binding/cleaving specificity exhibited by derivatives of **1**, (2) demonstrate that chiral derivatives of **1** exhibit enantiospecific recognition of DNA, and (3) indicate orientations relative to DNA from which **1** and its derivatives produce DNA cleavage.

Results

Synthesis and Characterization. Substituted derivatives of the parent ligand $SalenH_2$ were prepared by condensation of salicylaldehyde derivatives with ethylenediamine. Where not commercially available, substituted salicylaldehydes were prepared via the Reimer−Tiemann reaction[10] or through lithium aluminum hydride reduction followed by manganese dioxide oxidation of a substituted salicylic acid. Stirring the Schiff base ligands with $Mn(OAc)_2$ under aerobic conditions afforded the requisite Mn(III) complexes.[11] One set of derivatives studied were those bearing symmetrical substitutions of fluoro, chloro, bromo, nitro, methyl, *tert*-butyl, methoxy, or diethylamino groups at the 3,3′-, 4,4′-, 5,5′-, or 6,6′-positions (**2**−**14**, **19**, and **20**; Table 1), phenyl or methyl substituents at the 7,7′-imine positions (**15**−**17**), and the naphthalene analog **18**. In another set of derivatives, the 1,2-ethane bridge was replaced with 1,3-propane (**21**), 1,2-phenyl (**22**), (*R*,*R*)-, (*S*,*S*)-, or *meso*-1,2-cyclohexane (**23**), or (*R*,*R*)- or (*S*,*S*)-1,2-diphenylethane (**24**) linkages (Table 2). The complexes were characterized by spectroscopic methods (FT-IR, UV−vis, FAB-MS), melting (decomposition) point measurements, magnetic susceptibility measurements, elemental analysis, and optical rotation where appropriate.

DNA Affinity Cleaving.[12] Scheme 1 outlines our general approach to characterizing the DNA binding/cleaving properties of $[SalenMn^{III}]^+$ derivatives. DNA double-strand affinity cleaving was used to screen for DNA binding/cleaving activity, to determine relative cleavage efficiencies, and to define cleavage specificity at a resolution of 25−50 base pairs. This was followed by high-resolution analysis of cleavage patterns

Table 2. (Chiral) Bridge-Substituted $[SalenMn^{III}]^+$ Derivatives

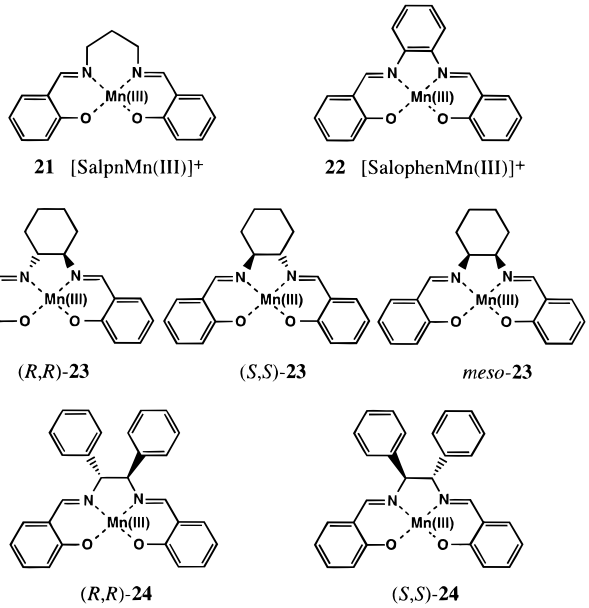

21 [SalpnMn(III)]$^+$ **22** [SalophenMn(III)]$^+$

(*R*,*R*)-**23** (*S*,*S*)-**23** *meso*-**23**

(*R*,*R*)-**24** (*S*,*S*)-**24**

Scheme 1

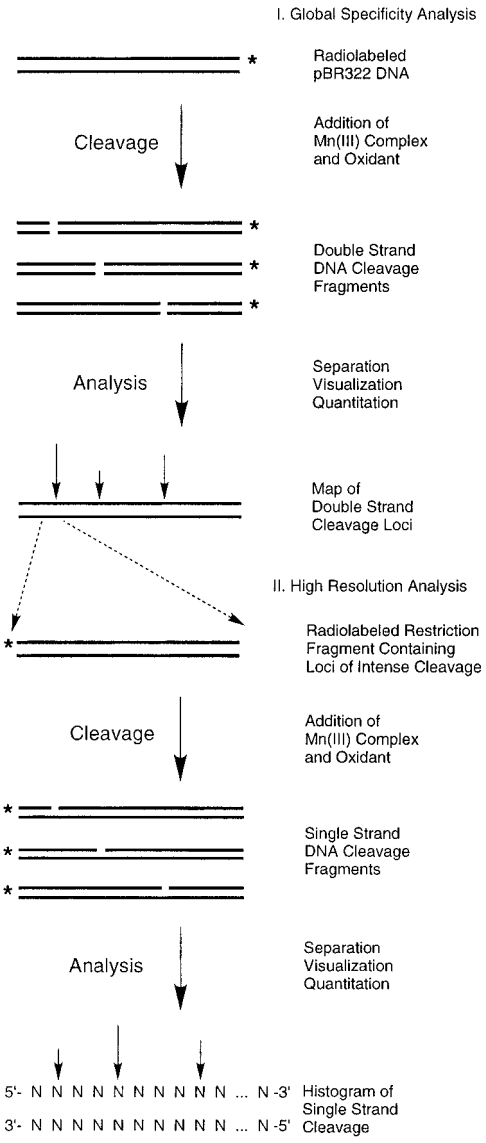

(10) Postmus, C., Jr.; Kaye, I. A.; Craig, C. A.; Matthews, R. S. *J. Org. Chem.* **1964**, *29*, 2693−2698.
(11) Zhang, W.; Jacobsen, E. N. *J. Org. Chem.* **1991**, *56*, 2296−2298.
(12) (a) Schultz, P. G.; Taylor, J. S.; Dervan, P. B. *J. Am. Chem. Soc.* **1982**, *104*, 6861−6863. (b) Taylor, J. S.; Schultz, P. G.; Dervan, P. B. *Tetrahedron* **1984**, *40*, 457−465. (c) Dervan, P. B. *Science* **1986**, *232*, 464−470.

produced on restriction fragments containing loci of intense double-strand cleavage.

Substrates for the affinity cleaving studies were derived from plasmid pBR322 (4363 base pairs, bp). For the double-strand cleavage assays, pBR322 was linearized with *Sty*I, which cleaves this plasmid at position 1369 within the sequence 5′-C/CTTGG-3′. Given the nonpalindromic nature of this cleavage site, it was possible to independently label the linearized plasmid at each of the resulting unique recessed 3′ ends by filling them in with either α-^{32}P dATP (bottom strand) or α-^{32}P TTP (top strand) using the Klenow fragment of DNA polymerase. Following incubation of these substrates with **1** and its derivatives in the presence and absence of terminal oxidants, products of DNA double-strand cleavage were resolved by electrophoresis on 1% agarose gels and visualized by autoradiography. The substrates for the high-resolution cleavage assays were 3′- and 5′-^{32}P end labeled, 517 bp *Eco*RI/*Rsa*I restriction fragments from pBR322 (spanning positions 3849−4361 on pBR322). The products of cleavage of these substrates were separated to nucleotide resolution by electrophoresis on denaturing polyacrylamide sequencing gels and visualized by autoradiography.

Double-Strand Cleavage Competency and Efficiency of Ring- and Imine-Substituted Derivatives. It was found that complexes **11** and **13**−**18**, which bear ether, amine, or aryl ring substituents and/or substituents at the imine positions, did not produce observable double-strand DNA cleavage by themselves or in the presence of millimolar concentrations of magnesium monoperoxyphthalate or potassium peroxymonosulfate. (These terminal oxidants do not produce significant DNA cleavage in the absence of metal complexes.[1]) Double-strand cleavage was effected by combinations of terminal oxidant with complexes **1**−**10**, which bear net electron-withdrawing halogen or nitro groups, and by **12**, which bears methoxy groups at the 4,4′-positions. The efficiency with which complexes **1**−**10** and **12** produced double-strand DNA cleavage varied significantly, as illustrated by the concentrations required to achieve comparable levels of cleavage in the presence of 1 mM magnesium monoperoxyphthalate after a reaction time of 1 h at 37 °C (Figure 1). Complexes **9** (5,5′-Br_2), **6** (5,5′-Cl_2), and **5** (4,4′-Cl_2) cleave with greater efficiency than does the parent complex **1**, complex **10** (5,5′-$(NO_2)_2$) cleaves with efficiency similar to that of **1**, and complexes **3** (5,5′-F_2), **2** (3,3′-F_2), **7** (6,6′-Cl_2), **4** (3,3′-Cl_2), **8** (3,3′,5,5′-Cl_4), and **12** (4,4′-$(OCH_3)_2$) cleave with diminishing efficiency. For the series of dichloro derivatives **4**−**8**, substituents at the 5,5′- or 4,4′-positions afford enhanced DNA binding/cleaving efficiencies relative to that of **1**, while substitution at the 6,6′-, 3,3′-, or (3,3′ + 5,5′)-positions leads to cleaving efficiencies that are lower than that of **1** and decrease in the order listed. For derivatives **3**, **6**, **9**, **10**, and **13**, which bear different substituents at the 5,5′-positions, DNA binding/cleaving efficiency is greatest for the dibromo and dichloro derivatives, similar to **1** for the dinitro derivative, somewhat reduced relative to **1** for the difluoro derivative, and greatly reduced (undetectable) for the dimethoxy derivative. The relationship between the identity of the substituent at a given position and the ordering of DNA binding/cleaving efficiencies is not general. The 3,3′-difluoro derivative **2** cleaves DNA more efficiently than does the 3,3′-dichloro derivative **4**. Complexes **19** and **20** were not tested for DNA double-strand cleavage activity, but they did produce efficient single-strand cleavage (see below).

Cleavage Specificity of Ring- and Imine-Substituted Derivatives. The identity and position of attachment of ring and imine substituents had no observable effect on DNA double-strand cleavage specificity—patterns of cleavage produced by **2**−**10** and **12** were, at this level of resolution, indistinguishable

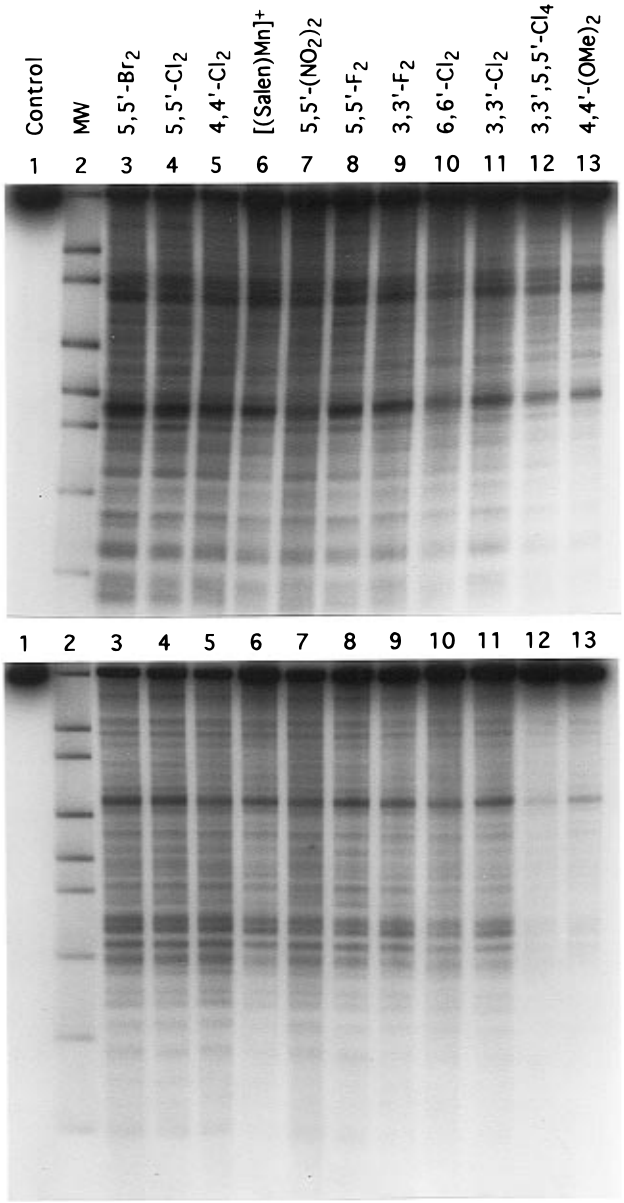

Figure 1. Autoradiographs of DNA double-strand cleavage patterns produced by ring- and imine-substituted [SalenMn^{III}]$^+$ complexes on *Sty*I-linearized, ^{32}P end labeled pBR322 plasmid DNA in the presence of 1.0 mM magnesium monoperoxyphthlate and resolved by electrophoresis on a 1% agarose gel. Top: 3′-^{32}P dATP end labeled DNA. Bottom: 3′-^{32}P TTP end labeled DNA. Lane 1, DNA incubated in the absence of metal complex or oxidant; lane 2, pBR322 molecular weight markers from pBR322 4365, 3371, 2994, 2368, 1998, 1768, 1372, 995, and 666 bp in length; lane 3, 5,5′-Br_2 (**9**, 12.5 μM); lane 4, 5,5′-Cl_2 (**6**, 12.5 μM); lane 5, 4,4′-Cl_2 (**5**, 15 μM); lane 6, [SalenMn^{III}]$^+$ (**1**, 20 μM); lane 7, 5,5′-$(NO_2)_2$ (**10**, 30 μM); lane 8, 5,5′-F_2 (**3**, 50 μM); lane 9, 3,3′-F_2 (**2**, 50 μM); lane 10, 6,6′-Cl_2 (**7**, 50 μM); lane 11, 3,3′-Cl_2 (**4**, 100 μM); lane 12, 3,3′,5,5′-Cl_4 (**8**, 100 μM); lane 13, 4,4′-$(OCH_3)_2$ (**12**, 100 μM).

from that of **1**. The observed cleavage loci correspond to regions of pBR322 containing sites of multiple, contiguous A:T base pairs, and the loci of greatest cleavage intensity correspond to the most A:T rich regions of the plasmid (Table 3).

The specificity of DNA cleavage by active derivatives of **1** was then probed at nucleotide resolution using *Eco*RI/*Rsa*I restriction fragments from pBR322 which contained the series of intense cleavage loci spanning positions 4164−4331 on pBR322. In the autoradiograph shown in Figure 2, complexes **1**−**10** and **12** have been grouped in order to emphasize the phenomenon that *substituents alter the precise patterns of cleavage produced by [SalenMn^{III}]$^+$ derivatives in a position specific but substituent independent fashion.* Complexes **2** and

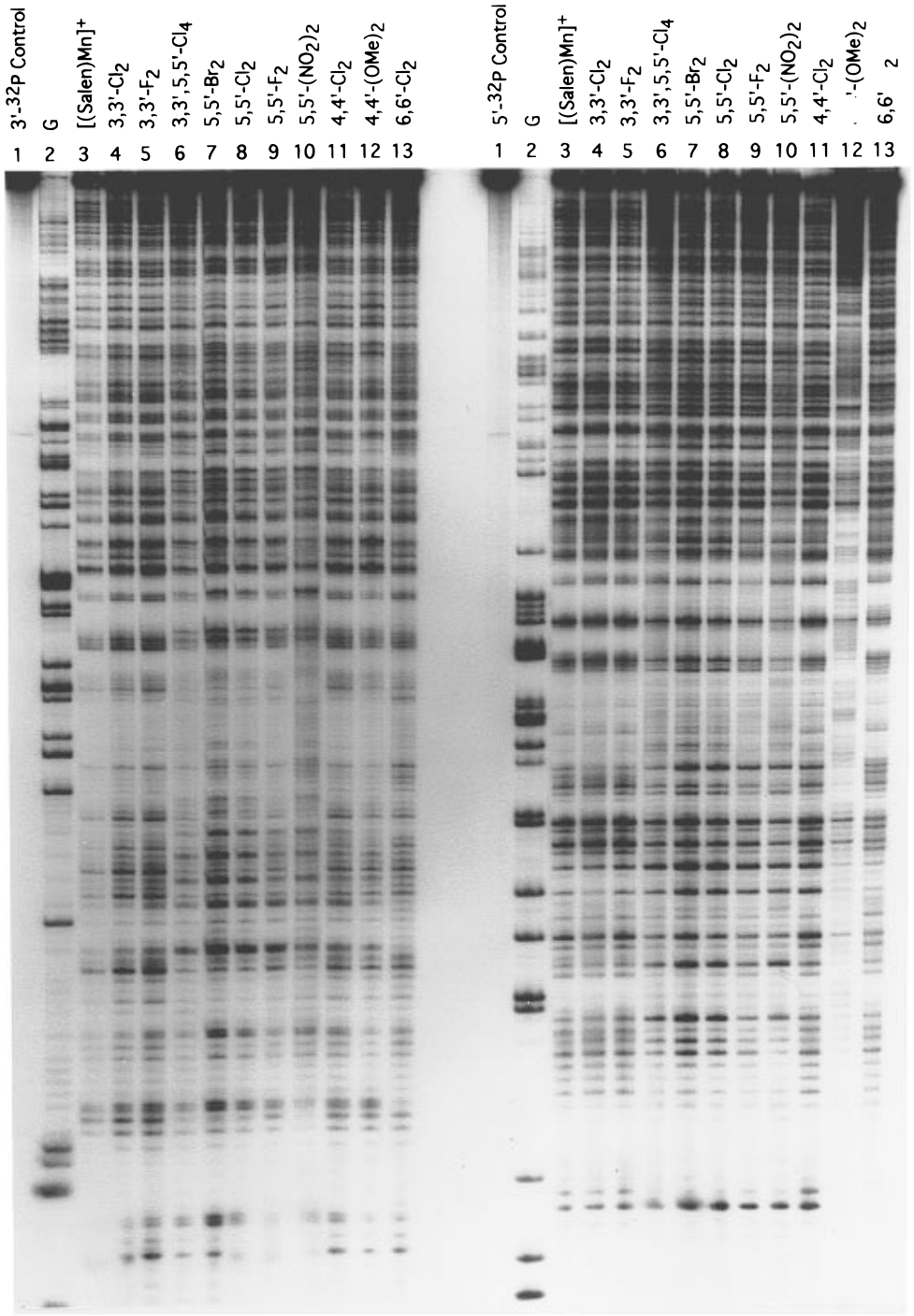

Figure 2. Autoradiograph of DNA single-strand cleavage patterns produced by ring- and imine-substituted $[SalenMn^{III}]^+$ complexes on 3′- and 5′-^{32}P end labeled 517 bp restriction fragments (*Eco*RI/*Rsa*I) from pBR322 plasmid DNA in the presence of 1.0 mM magnesium monoperoxyphthlate. Cleavage patterns were resolved on a 1:20 cross-linked 8% polyacrylamide/45% urea denaturing gel. Left set of lanes: 3′-^{32}P end labeled DNA. Right set of lanes: 5′-^{32}P end labeled DNA. For each set of lanes: lane 1, DNA incubated in the absence of metal complex or oxidant; lanes 2, Maxam−Gilbert chemical sequencing G reaction; lane 3, $[SalenMn^{III}]^+$ (**1**, 20 μM); lane 4, 3,3′-Cl_2 (**4**, 100 μM); lane 5, 3,3′-F_2 (**2**, 50 μM); lane 6, 3,3′,5,5′-Cl_4 (**8**, 100 μM); lane 7, 5,5′-Br_2 (**9**, 12.5 μM); lane 8, 5,5′-Cl_2 (**6**, 12.5 μM); lane 9, 5,5′-F_2 (**3**, 50 μM); lane 10, 5,5′-$(NO_2)_2$ (**10**, 30 μM); lane 11, 4,4′-Cl_2 (**5**, 15 μM); lane 12, 4,4′-$(OCH_3)_2$ (**12**, 100 μM); lane 13, 6,6′-Cl_2 (**7**, 50 μM).

4, with fluoro or chloro substituents in the 3,3′-positions, produce a cleavage pattern that matches that of **1**. Complexes **3**, **6**, **9**, and **10**, which bear halogen or nitro substituents in the 5,5′-positions, produce a common cleavage pattern which differs from that produced by **1**, **2**, or **4**. Tetrachloro derivative **8**, with substituents in the 3,3′- and 5,5′-positions, produces a pattern of cleavage which matches that of **3**, **6**, **9**, and **10**. Complexes **5** and **7**, with chloro substituents in the 4,4′- and 6,6′-positions, respectively, generate unique cleavage patterns. Some subtle differences are noted in the cleavage patterns produced by **5** and the 4,4′-dimethoxy analog **12**, but these patterns are more similar to one another than they are to that of any other derivative. Relative DNA binding/cleaving efficiencies observed in these experiments, which report single-strand cleavage, matched those determined by DNA double-strand affinity cleaving.

The efficiency and specificity of DNA cleavage by the 5,5′-dimethyl derivative **19** and the 5,5′-dibromo-3,3′-di-*tert*-butyl derivative **20** were also determined by high-resolution affinity cleaving (Figure 3). Complex **19** cleaves DNA with an efficiency similar to that of complexes **4** and **8** (i.e., with significantly less efficiency than **1**). Complex **19** bears electron-donating methyl substituents and produces a pattern of cleavage which is similar but not identical to the patterns of cleavage

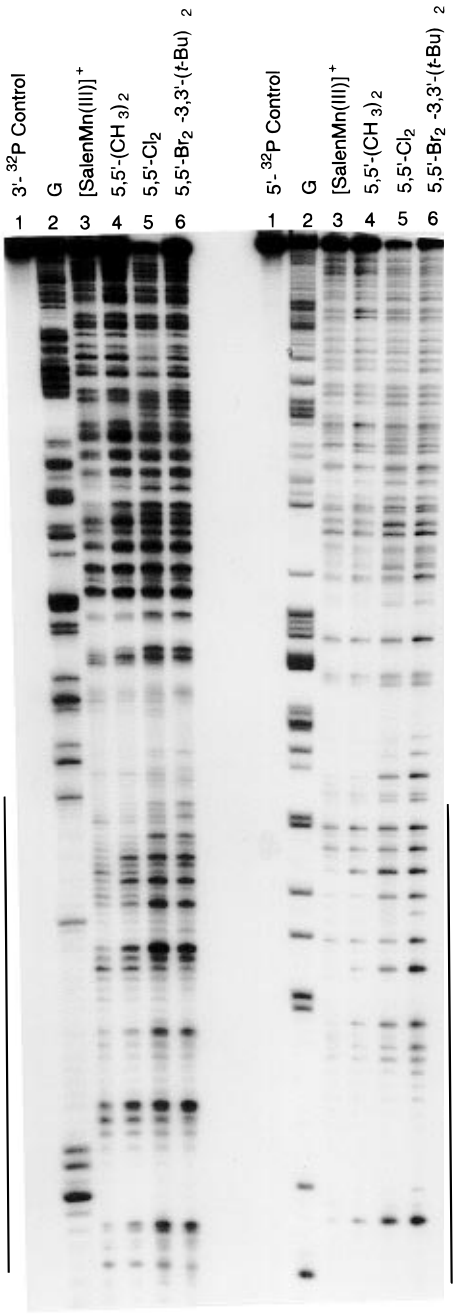

Figure 3. Autoradiograph of DNA single-strand cleavage patterns produced by ring-substituted [SalenMn^{III}]$^{+}$ complexes on 3′- and 5′-^{32}P end labeled 517 bp restriction fragments (*Eco*RI/*Rsa*I) from pBR322 plasmid DNA in the presence of 1.0 mM magnesium monoperoxyphthalate. Cleavage patterns were resolved on a 1:20 cross-linked 8% polyacrylamide/45% urea denaturing gel. Left set of lanes: 3′-^{32}P end labeled DNA. Right set of lanes: 5′-^{32}P end labeled DNA. For each set of lanes: lane 1, DNA incubated in the absence of metal complex or oxidant; lane 2, Maxam−Gilbert chemical sequencing G reaction; lane 3, [SalenMn^{III}]$^{+}$ (**1**, 20 μM); lane 4, 5,5′-CH_3 (**19**, 100 μM); lane 5, 5,5′-Cl_2 (**6**, 12.5 μM); lane 6, 5,5′-Br_2-3,3′-*tert*-Bu_2 (**20**, 20 μM).

produced by **6** and other complexes substituted with electron-withdrawing substituents in the 5,5′-positions. Complex **20** cleaves DNA more efficiently than **1** but less efficiently than the 5,5′-Br_2 derivative **9**. As was observed with the 3,3′,5,5′-tetrachloro derivative **8**, complex **20** exhibits DNA cleavage specificity which differs from that of **1** and the 3,3′-disubstituted derivatives **2** and **4**, yet matches that of complexes **3**, **6**, **9**, and **10**.

The autoradiographs shown in Figures 2 and 3 were quantified by densitometry, and these data were used to construct histograms of the DNA cleavage observed in the lower regions

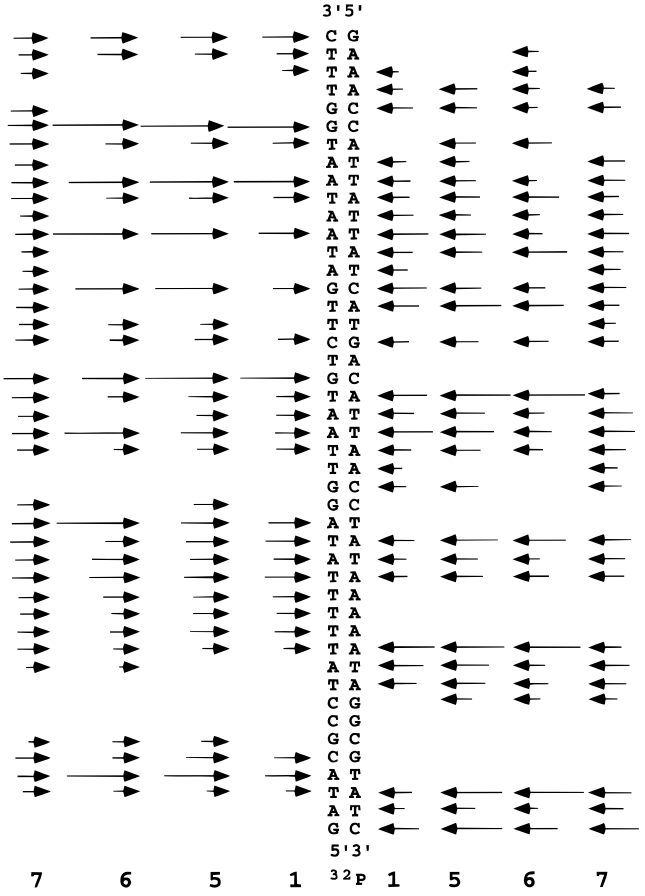

Figure 4. Representative histograms of single-strand DNA cleavage produced by ring- and imine-substituted [SalenMn^{III}]$^{+}$ derivatives in the presence of 1.0 mM magnesium monoperoxyphthlate on the 517 bp restriction fragments (*Eco*RI/*Rsa*I) from pBR322 plasmid DNA. Histograms were derived from densitometric analysis of the lower regions of the autoradiographs shown in Figure 2. Lengths of arrows correspond to the relative amounts of cleavage as determined by optical densitometry. Sequence positions of cleavage were determined by comparing the electrophoretic mobilities of DNA cleavage fragments to bands in Maxam−Gilbert chemical sequencing lanes.

Table 3. Loci of Greatest Double-Strand Cleavage Intensity Produced on *Sty*I-Linearized Plasmid pBR322 by [SalenMn^{III}]$^{+}$ and Derivatives

position[a,b]	sequence
3231	TTTTAAATTAAAAATGAAGTTTTAAAT-CAATCTAAAGTATATATT
4164	TTTTTCAATATTATTGAA
4228	TATTTAGAAAAATAAACAAATA
4315	ATTAACCTATAAAAATA

[a] Assignment made by interpolation from the sizes and migration distances of cleavage products relative to those of molecular weight standards. [b] Lowest numbered base pair of the underlined sequences, pBR322 numbering.

of the autoradiographs (Figures 4 and 5). The histograms show that complexes **2**−**10**, **12**, **19**, and **20**, similar to the unsubstituted parent complex, produce cleavage within and adjacent to sites of multiple contiguous A:T base pairs. However, intensities of cleavage at each nucleotide within the A:T target sequences produced by derivatives substituted in different ring positions differ by up to a factor of 4. The histograms also show that the cleavage patterns are shifted to the 3′ side on one DNA strand relative to the other and that single sites of cleavage are observed at some locations while at other sites cleavage extends symmetrically or unsymmetrically over many nucleotides. The minimal sequence requirement for specific cleavage by **1** and its derivatives appears to be two contiguous A:T base pairs.

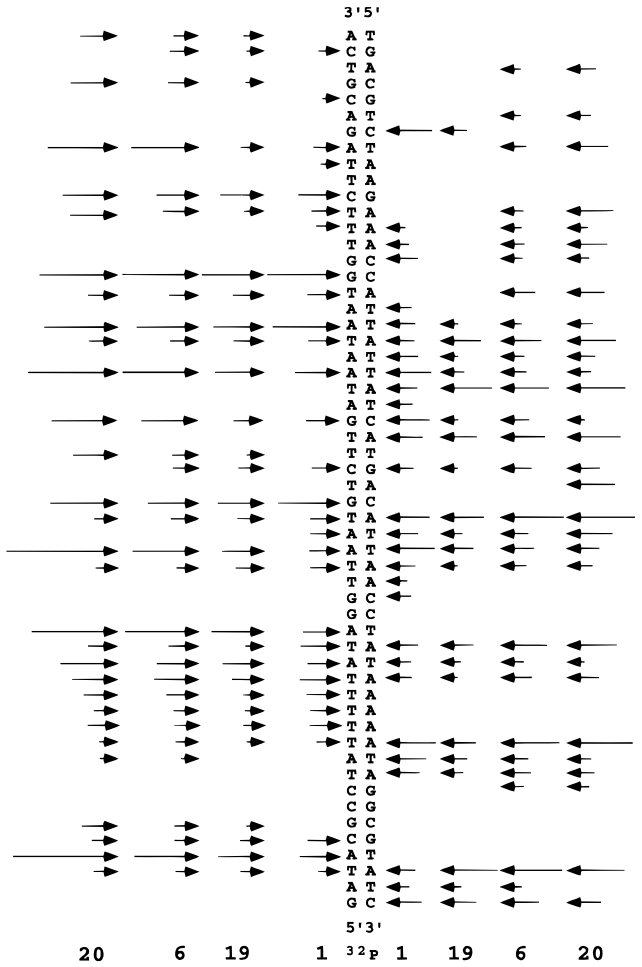

Figure 5. Histograms of single-strand DNA cleavage produced by ring-substituted $[SalenMn^{III}]^+$ derivatives in the presence of 1.0 mM magnesium monoperoxyphthlate on the 517 bp restriction fragments (*Eco*RI/*Rsa*I) from pBR322 plasmid DNA. Histograms were derived from densitometric analysis of the lower regions of the autoradiographs shown in Figure 3. Lengths of arrows correspond to the relative amounts of cleavage as determined by optical densitometry. Sequence positions of cleavage were determined by comparing the electrophoretic mobilities of DNA cleavage fragments to bands in Maxam−Gilbert chemical sequencing lanes.

Cleavage Competency and Efficiency of Bridge-Substituted Derivatives. Diphenyl-substituted derivatives (*R*,*R*)-**24** and (*S*,*S*)-**24** did not generate observable DNA cleavage. The bridge-substituted derivatives **21**−**23** were found to produce DNA cleavage in the presence of terminal oxidants, albeit with reduced efficiency relative to the parent complex **1**. This can be illustrated by the concentrations required to achieve similar levels of DNA double-strand cleavage in the presence of 1 mM magnesium monoperoxyphthalate after a reaction time of 1 h at 37 °C or by the differing extents of cleavage observed using equal concentrations of the agents (Figure 6). *The ability to cleave DNA was found to vary with the configuration of the complex, as cleavage efficiency decreased in the order (R,R)-23 > meso-23 > (S,S)-23*. In addition, it was found that **21** ($[SalpnMn^{III}]^+$) exhibited greatly reduced DNA binding/cleaving efficiency relative to **1**, while **22** ($[SalophenMn^{III}]^+$) produced DNA cleavage at a level intermediate between that of **1** and **21**. Considering all of the bridge-substituted derivatives, cleavage efficiency decreases in the order **1** > (*R*,*R*)-**23** > **22** > *meso*-**23** > (*S*,*S*)-**23** > **21** ≫ (*R*,*R*)-**24**, (*S*,*S*)-**24**.

Cleavage Specificity of Bridge-Substituted Derivatives. As with the ring-substituted derivatives, **21**−**23** produced patterns of DNA double-strand cleavage that were indistinguishable from that of **1**, with cleavage loci of greatest intensity mapping to

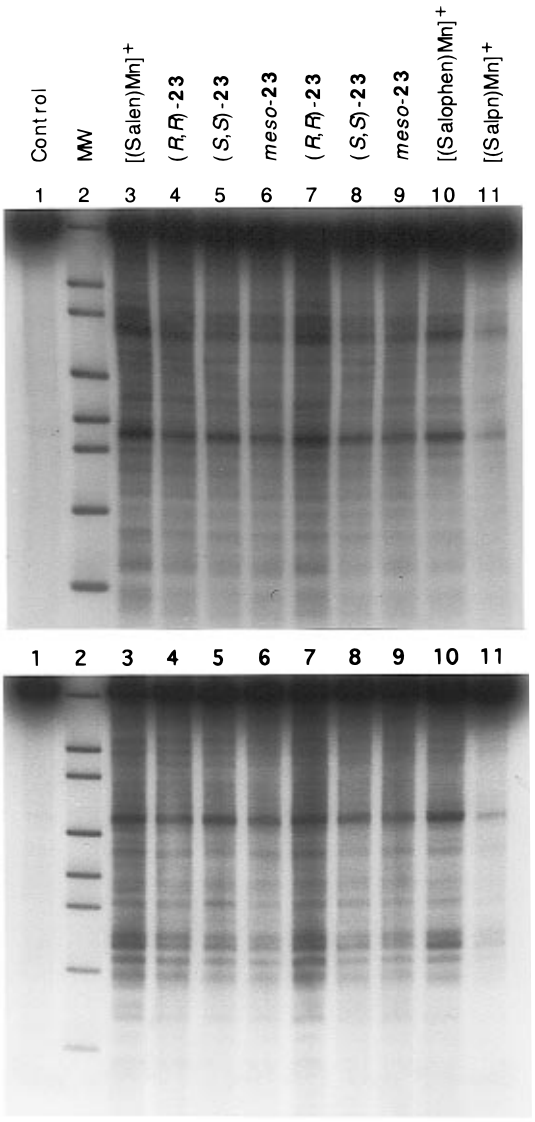

Figure 6. Autoradiographs of DNA double-strand cleavage patterns produced by bridge-substituted $[SalenMn^{III}]^+$ complexes on *Sty*I-linearized, ^{32}P end labeled pBR322 plasmid DNA in the presence of 1.0 mM magnesium monoperoxyphthlate and resolved by electrophoresis on a 1% agarose gel. Top: 3′-^{32}P dATP end labeled DNA. Bottom: 3′-^{32}P TTP end labeled DNA. Lane 1, DNA incubated in the absence of metal complex or oxidant; lane 2, pBR322 molecular weight markers from pBR322 4365, 3371, 2994, 2368, 1998, 1768, 1372, 995, and 666 bp in length; lane 3, $[SalenMn^{III}]^+$ (**1**, 20 μM); lane 4, (*R*,*R*)-**23**(20 μM); lane 5, (*S*,*S*)-**23** (100 μM); lane 6, *meso*-**23** (50 μM); lane 7, (*R*,*R*)-**23** (50 μM); lane 8, (*S*,*S*)-**23** (50 μM); lane 9, *meso*-**23** (50 μM); lane 10, $[SalophenMn^{III}]^+$ (**22**, 50 μM); lane 11, $[SalpnMn^{III}]^+$ (**21**, 100 μM).

A:T rich regions of pBR322 (Table 3). The 3′- and 5′-^{32}P end labeled, 517 bp *Eco*RI/*Rsa*I restriction fragments from pBR322 and DNA sequencing gels were then used to probe the specificity of single-strand DNA cleavage by **21**−**23** at nucleotide resolution. The DNA affinity cleaving data shown in Figure 7 demonstrate that the *patterns of cleavage produced by [SalenMn^{III}]$^+$ derivatives depend on both the structure and stereochemistry of the bridge*. Complexes **21**−**23** produce single-strand DNA cleavage patterns that do not match one another, those produced by the parent complex **1**, or those of the other complexes examined.

Histograms of DNA cleavage patterns produced by **21**−**23** (Figure 8) reveal that complexes **21**−**23**, like **1**, produce cleavage within and adjacent to sites of multiple contiguous A:T base pairs. Also, cleavage patterns produced by **21**−**23** are shifted to the 3′ side on one DNA strand relative to the other and consist of single sites of cleavage at some positions

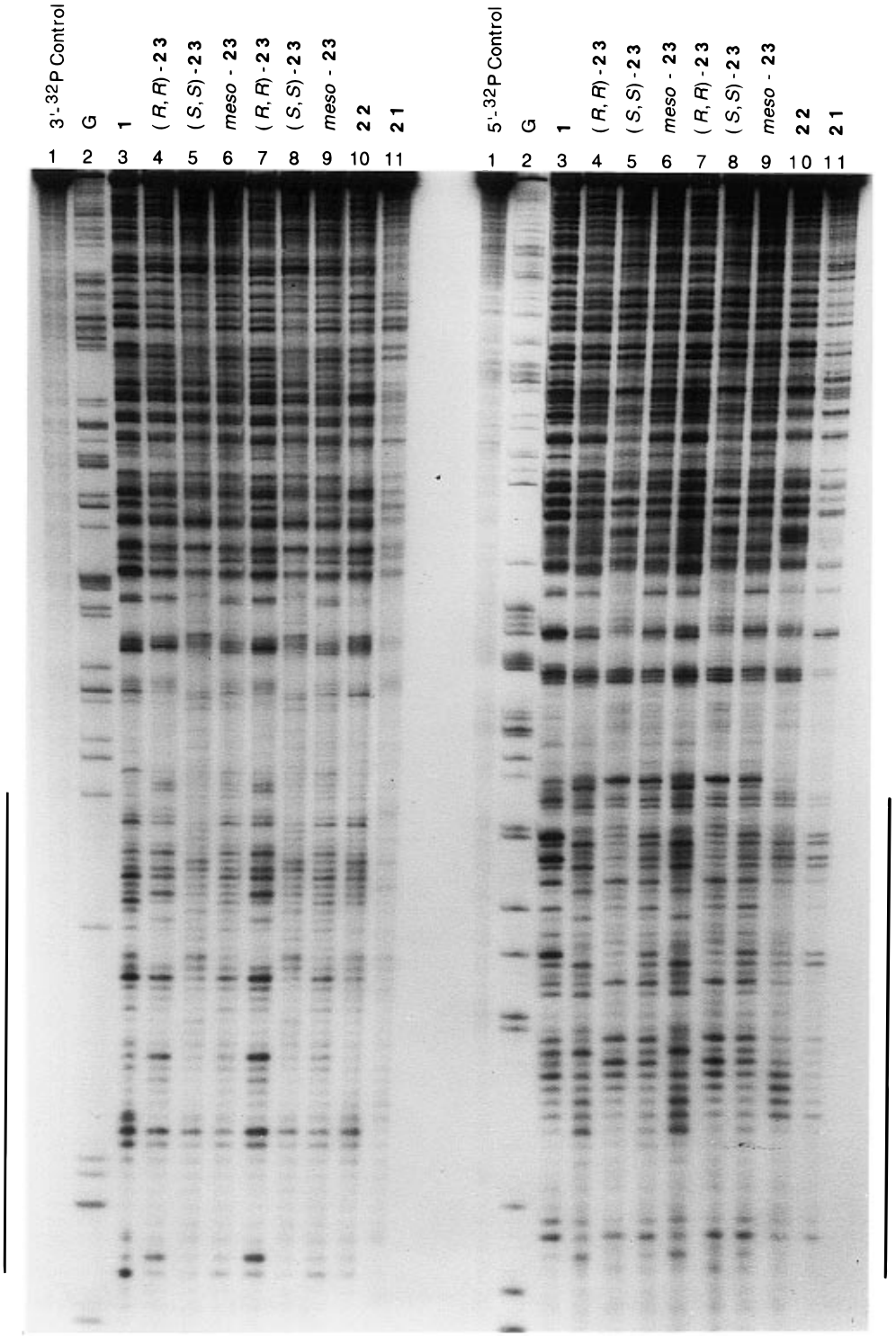

Figure 7. Autoradiograph of DNA single-strand cleavage patterns produced by bridge-substituted [SalenMn^{III}]$^{+}$ complexes on 3′- and 5′-^{32}P end labeled 517 bp restriction fragments (*Eco*RI/*Rsa*I) from pBR322 plasmid DNA in the presence of 1.0 mM magnesium monoperoxyphthlate. Cleavage patterns were resolved on a 1:20 cross-linked 8% polyacrylamide/45% urea denaturing gel. Left set of lanes: 3′-^{32}P end labeled DNA. Right set of lanes: 5′-^{32}P end labeled DNA. For each set of lanes: lane 1, DNA incubated in the absence of metal complex or oxidant; lanes 2, Maxam−Gilbert chemical sequencing G reaction; lane 3, [SalenMn^{III}]$^{+}$ (**1**, 20 μM); lane 4, (*R*,*R*)-**23** (20 μM); lane 5, (*S*,*S*)-**23** (100 μM); lane 6, *meso*-**23** (50 μM); lane 7, (*R*,*R*)-**23** (50 μM); lane 8, (*S*,*S*)-**23** (50 μM); lane 9, *meso*-**23** (50 μM); lane 10, [SalophenMn^{III}]$^{+}$ (**22**, 50 μM); lane 11, [SalpnMn^{III}]$^{+}$ (**21**, 100 μM).

while at other sites cleavage extends symmetrically or unsymmetrically over many nucleotides. Unlike ring-substituted [SalenMn^{III}]$^{+}$ derivatives wherein complexes containing different substituents at the same position display nearly identical cleavage patterns, the cleavage patterns of complexes **21**−**23** are each unique. Within a given A:T target sequence, cleavage intensities at individual nucleotides differ by up to a factor of 10 for **1** and **21**−**23**.

UV−Vis Analysis of Complex Stability and Activation. All of the [SalenMn^{III}]$^{+}$ derivatives exhibited UV−vis spectra typical of this family of complexes.[2] The spectra of some derivatives showed little change after incubation for 1 week in the aqueous buffer used for DNA cleavage reactions, while others (complexes **2**, **4**, **10**, **12**, **13**, **17**, **18**, **21**, and **22**) showed more pronounced changes. For example, after 1 week the phenyl-bridged complex **22** displayed greater than 30% loss of absorbance throughout most of the UV−vis region with the emergence of a new absorbance maximum at 258 nm. The 3,3′-

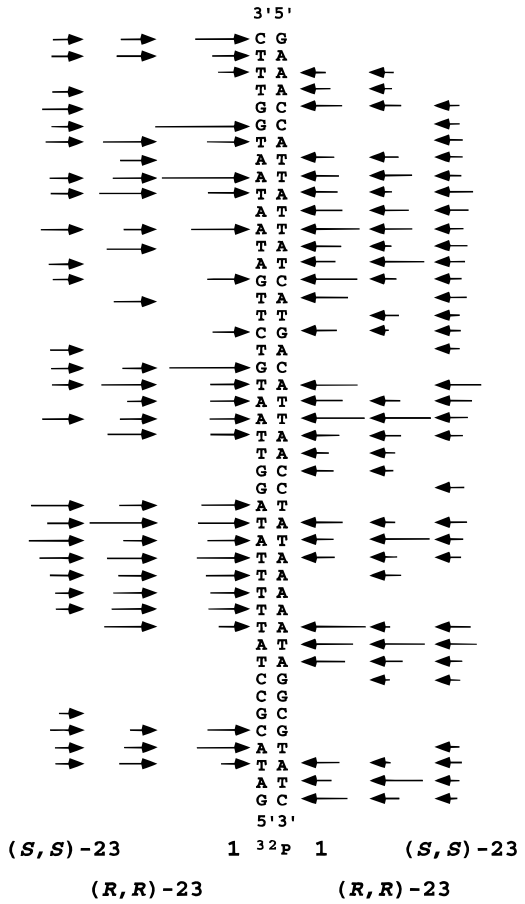

Figure 8. Histograms of single-strand DNA cleavage produced by **1** and chiral bridge-substituted $[SalenMn^{III}]^+$ complexes in the presence of 1.0 mM magnesium monoperoxyphthlate on the 517 bp restriction fragments (*Eco*RI/*Rsa*I) from pBR322 plasmid DNA. Histograms were derived from densitometric analysis of the lower regions of the autoradiographs shown in Figure 7, lanes 3−5. Lengths of arrows correspond to the relative amounts of cleavage as determined by optical densitometry. Sequence positions of cleavage were determined by comparing the electrophoretic mobilities of DNA cleavage fragments to bands in Maxam−Gilbert chemical sequencing lanes.

dichloro derivative **4** displayed reduced absorbance below 300 nm and increased absorbance at 400 nm with the loss of an absorbance maximum. When treated with magnesium monoperoxyphthalate, each of the complexes exhibiting DNA cleavage activity (except **21**) showed the increased absorption in the visible region which characterizes oxidatively activated **1**.[2] Among the derivatives which do not exhibit DNA binding/cleaving activity, complexes **13**, **15**, and **24** showed spectral changes consistent with oxidative activation in the presence of magnesium monoperoxyphthalate, while the spectra of complexes **16**−**18** and **22** showed little change upon addition of the oxidant. The spectral changes observed upon addition of the oxidant decayed over a period of minutes to afford spectra similar to those of the unactivated complexes, though of lesser intensity. In the case of complex **21**, this reduction in absorption intensity was observed immediately after addition of oxidant.

Discussion

Substituents alter both the steric and electronic properties of metal complexes, and in the case of DNA binding/cleaving metal complexes such as **1**, these could lead to changes in (1) the stability in aqueous buffered solution of the complexes or oxidatively activated intermediates derived from them, (2) the ability of activated intermediates to bind to target sites for cleavage in a productive fashion, and/or (3) the rates at which the complexes are oxidatively activated or at which oxidatively activated species mediate DNA cleavage. These changes could in turn be manifested as changes in the properties that we have addressed in the present study: DNA cleavage efficiency and specificity. The contributions of individual effects to the observed behavior, and the steric and electronic factors from which they are ultimately derived, may be difficult to distinguish since they may act in concert or in opposition through multiple mechanisms. However, consideration of results obtained with a series of related derivatives, including stereoisomers, can provide insight into the determinants involved.[6−9] This approach has been facilitated in the present study by the ease of synthesis of $[SalenMn^{III}]^+$ derivatives.

Binding Location and Cleavage Mode. When examined at high resolution, the cleavage patterns produced by all active derivatives were found to be shifted to the 3′ end on one DNA strand relative to the other. These results indicate that cleavage occurs from the minor groove of right-handed double-helical DNA.[12] The observed nonuniform patterns of cleavage and structure dependent differences in cleavage patterns are consistent with a process involving a specifically bound rather than a freely diffusible reactive species such as hydroxyl radical.[12,13] This latter point is compellingly demonstrated by the finding that the enantiomeric complexes (*R*,*R*)-**23** and (*S*,*S*)-**23** cleave DNA with different efficiencies and generate different cleavage patterns.

Cleavage Efficiency: Ring- and Imine-Substituted Derivatives. Seventeen of the 26 derivatives of complex **1** studied produced specific cleavage of DNA in the presence of terminal oxidants. No clear correlation was found between the UV−vis absorption behavior in the absence and the presence of oxidant and the DNA binding/cleaving properties of these complexes. Complexes **11** and **13** do not produce DNA cleavage, but UV−vis studies indicate that they are stable in reaction buffer, undergo activation in the presence of oxidant, and are not especially prone to decomposition upon activation. Thus, it appears that the inability of these complexes to effect DNA cleavage is due to the inability of their oxidatively activated forms to interact and/or react with DNA.

The results clearly indicate that the position of attachment and identity of substituents affect the ability of $[SalenMn^{III}]^+$ derivatives to effect DNA cleavage. The position of attachment is obviously important, since the regioisomeric dichloro derivatives exhibit both enhanced (**5** and **6**) and diminished (**4** and **7**) DNA cleavage efficiencies relative to that of **1**. With regard to substituent identity, the finding that **9** (5,5′-Br_2), **6** (5,5′-Cl_2), and **10** (5,5′-$(NO_2)_2$) cleave DNA with efficiencies equal to or greater than that of the parent complex **1** while **13** (5,5′-$(OCH_3)_2$) is inactive is in general accord with the results of Kochi et al., who found that **6** and **10** exhibited increased efficiency as catalysts for olefin epoxidation and carbon−hydrogen activation relative to the efficiencies of **1** and **13**.[2] The data for this series of derivatives cannot be explained by simple models in which either steric repulsion or favorable interactions between 5,5′-substituents and DNA dictate cleavage efficiency. Substituents at the 5,5′-positions strongly affect the redox properties of $[SalenMn^{III}]^+$ derivatives,[2,5] and it is likely that the great differences in DNA binding/cleaving efficiencies between complexes **9**, **6**, and **10** on the one hand and complexes **13** and **19** (5,5′-$(CH_3)_2$) on the other derive primarily from electronic effects associated with the presence of net electron-withdrawing bromo, chloro, or nitro groups versus net electron-donating methoxy or methyl groups at these positions. However, among

(13) (a) Hertzberg, R. P.; Dervan, P. B. *J. Am. Chem. Soc.* **1982**, *104*, 313−315. (b) Hertzberg, R. P.; Dervan, P. B. *Biochemistry* **1984**, *23*, 3934−3945. (c) Tullius, T. D.; Dombroski, B. A.; Churchill, M. E. A.; Kam, L. *Methods Enzymol.* **1987**, *155*, 537−558.

complexes bearing electron-withdrawing substituents in the 5,5′-positions, DNA binding/cleaving efficiency is not an unvarying function of the increasing electron-withdrawing character of the substituent. pK_a values and oxidation potentials of *para*-substituted methoxy-, methyl-, fluoro-, bromo-, chloro-, and nitrophenols[14] suggest that oxidation potentials for the Salen complexes will increase in the order **13** < **19** < **3** < **1** < **9** < **6** < **10**, yet DNA cleavage efficiency is observed to increase in the order **13** < **19** < **3** < **1** ≈ **10** < **9** ≈ **6**. A similar phenomenon was observed by Muller et al., who found that DNA oxidation by nickel complexes of tetraazamacrocyclic ligands increases with redox potential only up to a certain point.[9] For the series of 3,3′-substituted derivatives, DNA cleavage efficiency decreases with increasing size of hydrogen, fluoro, chloro, and methoxy substituents: **1** > **2** > **4** ≫ **11**. However, the fact that complex **20**, with bulky *tert*-butyl groups in the 3,3′-positions, exhibits DNA cleavage efficiency greater than that of **1** suggests that the DNA cleavage properties of these derivatives are not dictated by the steric nature of 3,3′-substituents. This notion is further supported by consideration of the cleavage specificity exhibited by these derivatives (see below).

Cleavage Efficiency: Bridge-Substituted Derivatives. Modifications on the bridge of [SalenMn^{III}]$^+$ also significantly affect the DNA cleavage efficiency. Differences between complexes **1** and **21** ([SalpnMn^{III}]$^+$) may derive from the additional flexibility imparted by the extra methylene unit. In general, Salen complexes form trans isomers with the phenolate oxygens and the imine nitrogens forming a plane; however, **21** can form trans or cis β conformers.[15] The cis β conformation of **21** readily forms the stable dioxo dimer [SalpnMn^{IV}O]$_2$ in the presence of base and oxidant. Formation of this or related species may account for the decreased cleavage efficiency of **21** relative to that of **1**.[16]

Due to the phenyl linkage, complex **22** should exhibit increased rigidity relative to that of **1**. Complex **22** also has increased aromatic surface area which may participate in interactions with DNA by groove binding or perhaps even intercalation. ESR spectra of substituted Salen copper complexes bound to DNA fibers are consistent with a change in DNA binding mode from groove binding to intercalation upon changing the bridging ethylene group to phenylene or naphthalene groups.[17] However, manganese porphyrin complexes require axial ligands which sterically restrict the metalloporphyrin to DNA groove binding modes.[18] This combined with the finding that **22** displays A:T selective cleavage similar to that of **1** and the other derivatives leads us to conclude that minor groove binding rather than intercalation is the principal mode through which **22** produces DNA cleavage. The reduced cleaving efficiency of **22** versus **1** may arise from differential electronic factors associated with conjugating versus nonconjugating linkers and/or from steric interactions associated with the phenyl bridge which hinder approach of **22** to the DNA double helix in a cleavage competent orientation. The cleavage specificity results suggest that at least some derivatives of **1** produce DNA cleavage from an orientation in which the bridge of the complex is oriented toward or along the minor groove (see below). It is therefore possible that repulsive interactions between the phenyl bridge of activated **22** and the DNA target could result in diminution of cleavage efficiency for **22** relative to that for **1**.

(*R*,*R*)-, (*S*,*S*)-, and *meso*-**23** exhibit different DNA cleavage efficiencies, indicating that DNA recognition by activated forms of these complexes is both stereo- and enantioselective. Because the electronic properties of unbound (*R*,*R*)-**23** and (*S*,*S*)-**23** (and activated intermediates derived from them) are identical, the observed differences in cleavage efficiencies (5-fold for these enantiomeric complexes) must have their basis in diastereomeric interactions with DNA. If activated intermediates derived from **23** interact with DNA in a bridge first or side first fashion, then steric interactions between their cyclohexano bridges and the DNA minor groove which hinder the initiation of strand scission could account for the reduced cleavage efficiency for **23** relative to that for **1** as well as the observed stereoselectivity.

The diphenyl derivatives (*R*,*R*)-**24** and (*S*,*S*)-**24** do not produce observable DNA cleavage under the reaction conditions employed. However, since UV−vis analyses demonstrate that these complexes are stable in reaction buffer and yield spectral changes consistent with oxidative activation without considerable decomposition, it appears that DNA cleavage is inhibited by the inability of oxidatively activated forms of **24** to interact and/or react with DNA.

Cleavage Specificity: General. The substituents present in the cleavage competent complexes do not alter the proclivity of **1** to produce cleavage from the minor groove of right-handed double-helical DNA at sites containing multiple, contiguous A:T base pairs. This suggests a general shape selection mechanism[7,19] for DNA recognition by [SalenMn^{III}]$^+$ derivatives in which these planar cationic agents can be sandwiched within the electron rich,[20] relatively narrow minor groove found in A:T rich regions. Here they form stabilizing van der Waals interactions with deoxyribose residues of the DNA backbone but not highly specific contacts such as hydrogen bonds with the base pairs themselves. The protruding N2 amino group of guanine will preclude deep penetration into the minor groove by **1** and its derivatives at sequences containing G:C base pairs.

While substituents do not alter the general A:T specificity of **1**, substituents do change the patterns of cleavage produced within A:T rich target sites. These differences reflect substituent-induced changes in the relative rates of DNA cleavage at each nucleotide within A:T rich target sequences. The data do not allow us to distinguish whether these differences derive from changes in the relative affinities of activated intermediates for different binding/cleaving sites and/or from changes in rate constants for cleavage at the various sites.[21]

Cleavage Specificity: Chiral Bridge-Substituted Derivatives. Chiral derivatives of [SalenMn^{III}]$^+$ and structurally related species have been shown to be highly efficient catalysts for asymmetric epoxidation,[5,11,22] aziridination,[23] aldol,[24] sulfide oxidation,[25] and cyclopropanation reactions.[26] The observation that the enantiomeric complexes (*R*,*R*)-**23** and (*S*,*S*)-**23** produce different patterns of cleavage demonstrates *enantiospecificity* in DNA binding/cleaving. We believe that both the observed differences in binding/cleaving efficiencies and specificities arise from differences in nonbonded interactions between the diastereomeric complexes of activated (*R*,*R*)-**23**:DNA and activated (*S*,*S*)-**23**:DNA at individual sites of cleavage. While models indicate that (*R*,*R*)-**23** is twisted in a sense that is more

(14) Arnett, E. M.; Amarnath, K.; Harvey, N. G.; Venimadhavan, S. *J. Am. Chem. Soc.* **1990**, *112*, 7346−7353.
(15) Larson, E. J.; Pecoraro, V. L. *J. Am. Chem. Soc.* **1991**, *113*, 3810−3818.
(16) We have found that preformed [SalpnMn^{IV}O]$_2$ does not produce nicking of supercoiled plasmid DNA at 100 μM concentration in either the absence or presence of additional oxidant.
(17) Sato, K.; Chikira, M.; Fujii, Y.; Komatsu, A. *J. Chem. Soc., Chem. Commun.* **1994**, 625−626.
(18) (a) Pasternack, R. F.; Gibbs, E. S.; Villafranca, J. J. *Biochemistry* **1983**, *22*, 2406−2414. (b) Ward, B.; Skorobogaty, A.; Dabrowiak, J. C. *Biochemistry* **1986**, *25*, 7827−7833.
(19) (a) Lee, M. D.; Ellestad, G. A.; Borders, D. B. *Acc. Chem. Res.* **1991**, *24*, 235−243. (b) Uesugi, M.; Sugiura, Y. *Biochemistry* **1993**, *32*, 4622−4627. (c) Kahne, D. *Chem. Biol.* **1995**, *2*, 7−12.
(20) Pullman, B.; Lavery, R.; Pullman, A. *Eur. J. Biochem.* **1982**, *124*, 229−238.

complementary to the minor groove of B form DNA, further analysis and modeling studies will be needed to understand the detailed basis for these effects.

There is considerable precedent for differential DNA cleavage properties based on diastereomeric interactions between chiral small molecules and DNA. For example, enantiomers of intercalating tris(chelate) cobalt and rhodium complexes exhibit enantiospecific photocleavage of double-helical DNA.[7] In these systems, enantiospecificity is based on steric interactions between the DNA receptor and nonintercalated ligands on the metal complexes. The intrinsic site selectivity of these complexes may be significantly enhanced by addition of substituents to the nonintercalated ligands which participate in specific hydrogen bonding and van der Waals interactions with groups present in the major groove of B DNA.[7d−f] These enhancements in specificity were not observed in the present study, indicating that the specificity of the $[SalenMn^{III}]^+$ derivatives examined derives from general shape selective recognition alone.

Cleavage Specificity: Ring- and Imine-Substituted Derivatives. The patterns of cleavage produced by derivatives of **1** are dependent upon the position of substituents, but nearly independent of substituent identity. Complexes substituted in the 5,5′-positions with electron-withdrawing groups (**3**, **6**, **9**, and **10**) produce patterns of cleavage that are indistinguishable from one another, subtly different from the pattern of cleavage produced by the complex (**19**) which bears electron-donating methyl substituents in the 5,5′-positions, and more substantially different from the cleavage pattern produced by **1**, which has hydrogen substituents in the 5,5′-positions. Since **3**, **6**, **9**, and **10** bear substituents that are smaller than (fluoro), similar to (chloro), and larger than (bromo, nitro) a methyl group in size, we are led to conclude that the slight differences in specificity observed with **3**, **6**, **9**, and **10** versus **19** are due to electronic factors, but that the more substantial differences between **3**, **6**, **9**, **10**, and **19** versus **1** arise from steric factors. It is reasonable to expect that steric interactions between substituents and the DNA minor groove will perturb the rates of hydrogen abstraction at and/or thermodynamic partitioning among DNA binding/cleaving sites. It is somewhat puzzling that the smallest change in size from hydrogen (van der Waals radius = 1.20 Å) to fluorine (van der Waals radius = 1.47 Å) at the 5,5′-positions alters cleavage specificity, but that substitution of much larger chloro, bromo, or nitro groups does not lead to further changes in cleavage specificity. However, we note that a series of manganese and cobalt porphyrins exhibited no change in cleavage specificity when the steric bulk of substituents lying in the porphyrin plane was increased.[6b,c]

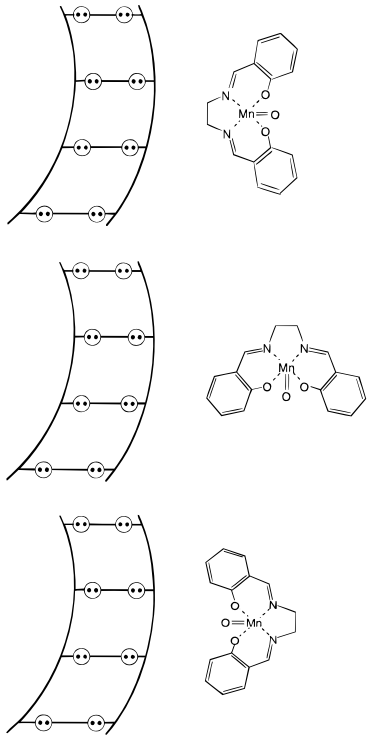

Figure 9. Models for possible reactive orientations for DNA cleavage by $[SalenMn^{V}O]^+$. Circles with two dots represent lone pairs of electrons on adenine N3 or thymine O2 atoms at the edges of the base pairs on the floor of the minor groove of B form DNA. Top: Bridge first approach of the complex to DNA. Middle: Side first approach of the complex to DNA. Bottom: Concave edge first approach of the complex to DNA. The data with derivatives substituted in the 3,3′-positions is inconsistent with the latter model.

The regioisomeric dichloro derivatives **4**−**7** generate different patterns of cleavage. We consider it likely that steric effects are also important in determining these differences, but more data will be needed to demonstrate this with certainty.

Reactive Orientation. The results obtained with derivatives bearing substituents in the 3,3′-positions (**2**, **4**, **8**, and **20**) provide insight into the orientation of cleavage competent intermediates derived from these complexes and **1** relative to DNA. The patterns of cleavage produced by **2** and **4** match those produced by **1**, suggesting that activated intermediates derived from these three complexes adopt a common reactive orientation when bound to DNA in which their concave edges, from which protrude the 3,3′-substituents, are not oriented toward the double helix. Sigman and co-workers observed no change in cleavage patterns produced by bis(1,10-phenanthroline):copper complexes substituted in the 5- or 6-positions and used these results to support a model for DNA complexation in which substituents at these positions extend away from the DNA helix.[8]

Three possible reactive orientations for the putative intermediate $[SalenMn^{V}O]^+$ are depicted in Figure 9: convex edge (bridge) first, side first, and concave edge first. The data for **1**, **2**, **4**, **8**, and **20** are consistent with either of the first two models but not with the third. That tetrasubstituted complexes **8** and **20** produce cleavage patterns similar to those produced by the 5,5′-disubstituted derivatives **3**, **6**, **9**, and **10** suggests that activated intermediates derived from the latter complexes also do not bind with their concave edges oriented toward the double helix. Bridge first or side first approaches are also consistent

(21) (a) Baker, B. F.; Dervan, P. B. *J. Am. Chem. Soc.* **1985**, *107*, 8266−8268. (b) Baker, B. F.; Dervan, P. B. *J. Am. Chem. Soc.* **1989**, *111*, 2700−2712. (c) De Voss, J. J.; Hangeland, J. J.; Townsend, C. A. *J. Am. Chem. Soc.* **1990**, *112*, 4554−4556. (d) Hurley, L. H.; Warpehoski, M. A.; Lee, C.-S.; McGovren, J. P.; Scahill, T. A.; Kelly, R. C.; Mitchell, M. A.; Wicnienski, N. A.; Gebhard, I.; Johnson, P. D.; Bradford, V. S. *J. Am. Chem. Soc.* **1990**, *112*, 4633−4649. (e) Wender, P. A.; Kelly, R. C.; Beckham, S.; Miller, B. L. *Proc. Natl. Acad. Sci. U.S.A.* **1991**, *88*, 8835−8839. (f) Myers, A. G.; Harrington, P. M.; Kwon, B.-M. *J. Am. Chem. Soc.* **1992**, *114*, 1086−1087. (g) Walker, S.; Landovitz, R.; Ding, W. D.; Ellestad, G. A.; Kahne, D. *Proc. Natl. Acad. Sci. U.S.A.* **1992**, *89*, 4608−4612. (h) Mah, S. C.; Townsend, C. A.; Tullius, T. D. *Biochemistry* **1994**, *33*, 614−621. (i) Myers, A. G.; Cohen, S. B.; Kwon, B.-M. *J. Am. Chem. Soc.* **1994**, *116*, 1255−1271. (j) Myers, A. G.; Cohen, S. B.; Kwon, B.-M. *J. Am. Chem. Soc.* **1994**, *116*, 1670−1682. (k) Chatterjee, M.; Cramer, K. D.; Townsend, C. A. *J. Am. Chem. Soc.* **1994**, *116*, 8819−8820.

(22) (a) Jacobsen, E. N.; Deng, L.; Furukawa, Y.; Martinez, L. E. *Tetrahedron* **1994**, *50*, 4323−4334. (b) Deng, L.; Jacobsen, E. N. *J. Org. Chem.* **1992**, *57*, 4320−4323.

(23) Li, Z.; Conser, K. R.; Jacobsen, E. N. *J. Am. Chem. Soc.* **1993**, *115*, 5326−5327.

(24) Carreira, E. M.; Singer, R. A.; Lee, W. *J. Am. Chem. Soc.* **1994**, *116*, 8837−8838.

(25) Sasaki, C.; Nakajima, K.; Kojima, M.; Fujita, J. *Bull. Chem. Soc. Jpn.* **1991**, *64*, 1318−1324.

(26) (a) Nozaki, H.; Takaya, H.; Moriuti, S.; Noyori, R. *Tetrahedron* **1968**, *24*, 3655−3669. (b) Aratani, T.; Yoneyoshi, Y.; Nagase, T. *Tetrahedron Lett.* **1977**, 2599−2602. (c) Aratani, T.; Yoneyoshi, Y.; Nagase, T. *Tetrahedron Lett.* **1982**, 685−688.

with the observation that bridge structure and stereochemistry affect both DNA binding/cleaving efficiency and specificity by complexes **21**−**23** and provide a rationale for the lack of cleavage by diphenyl derivatives (*R*,*R*)-**24** and (*S*,*S*)-**24**. Finally, when considered in light of concave edge away models, it is apparent that the diminished DNA binding/cleaving efficiency observed for complexes **2** and **4** relative to that of **1** derives from electronic rather than steric factors.

Bridge first and side first orientations bear some analogy to the geometries proposed for minor groove binding by enantiomers of tris(1,10-phenanthroline):ruthenium(II).[27] In contrast, the apparent preference for bridge first or side first orientations by activated intermediates derived from **1** and at least some of its derivatives differs from that observed with the crescent-shaped minor groove binding agents netropsin and distamycin. However, in the case of those bis- and tris(*N*-methylpyrrolecarboxamides), orientation of their concave edges toward the minor groove allows for formation of a series of hydrogen bonds between amide NHs and lone pair electrons from O2 atoms of thymine and N3 atoms of adenine.[12,28] No hydrogen bond donor groups are found on the concave edge of **1**; rather, this edge of the molecule displays hydrogen bond acceptor groups (i.e., lone pair electrons on the phenolate oxygen atoms that are ligated to the manganese ion).

Experimental Section

Synthesis of Substituted Salicylaldehydes. 5-Fluorosalicylaldehyde and 3-, 4-, and 6-chlorosalicylaldehyde were made by the Reimer−Tiemann method from the corresponding substituted phenols.[10] 5-Methylsalicylaldehyde was obtained by $LiAlH_4$ reduction of 5-methylsalicylic acid and subsequent MnO_2 oxidation.

General Method for Synthesis of Substituted [SalenMn^{III}]OAc Salts. The general method for synthesis of the Mn(III) complexes is typified by the procedure for the 3,3′-$(OCH_3)_2$ derivative **11**. To a solution of *o*-vanillin (326 mg, 2.14 mmol) in ethanol (2 mL) was added ethylenediamine (63.5 mg, 1.06 mmol) in ethanol (1 mL). The solution turned bright yellow, and a yellow precipitate was formed. The slurry was stirred and heated until homogeneous, whereupon a solution of manganese(II) acetate (224 mg, 0.91 mmol) in warm ethanol (2 mL) was added. The reaction mixture immediately became dark. After refluxing in the presence of air for 1 h, the mixture was cooled to room temperature and allowed to crystallize overnight (some complexes required the addition of ether to induce crystallization or precipitation). The product was filtered, washed with cold ethanol and diethyl ether, and dried in vacuo to afford 319 mg (0.85 mmol, 80%) of [*N*,*N*′-ethylenebis(3-methoxysalicylideneaminato)]manganese(III) acetate (**11**) as brown microcrystals, mp 198−200 °C (dec). FT-IR (cm^{-1}, film): 1629 (s), 1591 (s), 1566 (s), 1554 (s), 1536 (s), 1429 (s), 1395 (s), 1335 (m), 1296 (s), 1226 (m), 1190 (m), 1144 (s), 1087 (m), 1044 (m), 986 (w), 938 (m), 918 (w), 879 (w), 857 (m), 846 (m), 780 (m), 742 (m), 689 (m), 676 (m). UV−vis (H_2O) λ_{max} (ϵ, M^{-1} cm^{-1}): 402 (3700), 323 (9300), 301 (9400), 262 (13800), 225 (34200). UV−vis (buffer, fresh) λ_{max} (ϵ, M^{-1} cm^{-1}): 405 (4800), 323 (11100), 295 (13500), 262 (14600), 228 (37000). UV−vis (buffer, >1 week) λ_{max} (ϵ, M^{-1} cm^{-1}): 405 (4900), 323 (8400), 295 (11000), 262 (9300), 228 (29400). Anal. Calcd for $C_{21}H_{26}N_2O_{7.5}Mn$: C, 52.40; H, 5.44; N, 5.82. Found: C, 52.25; H, 5.47; N, 5.83. FAB-MS: calcd for $C_{18}H_{18}N_2O_4Mn$ ([3,3′-$(OCH_3)_2$SalenMn^{III}]$^+$) 381.1; found 381.1. μ_{eff} = 4.81.

UV−Vis Analysis. UV−vis spectra of complexes **1**−**24** were measured at a concentration of 50 μM in 40 mM Tris acetate pH 7.0 immediately after fresh preparation and after incubation at room temperature in the dark for 1 week. For the analysis of complex activation, spectra were taken before and at several time points after addition of 10 equiv of magnesium monoperoxyphthalate.

General Procedure for DNA Cleavage Reactions with Substituted [SalenMn^{III}]$^+$ Complexes. Three microliters of a substituted [SalenMn^{III}]$^+$ complex solution was added to 9 μL of a solution containing ^{32}P end labeled DNA restriction fragment[29] (10000−30000 cpm) and calf thymus DNA in Tris acetate buffer pH 7.0. DNA cleavage was initiated by the addition of 3 μL magnesium monoperoxyphthlate (MgMPP) solution. Final concentrations in 15 μL total volume were the following: substituted [SalenMn^{III}]$^+$ complex, as given in the figure legends; calf thymus DNA, 100 μM bp; Tris, 40 mM; MgMPP, 1.0 mM. DNA cleavage was allowed to proceed 1 h at 37 °C before DNA cleavage products were separated by gel electrophoresis. For studies of DNA double-strand cleavage, cleavage reactions were treated with 3 μL of 25% Ficoll loading buffer, loaded onto a 25 cm long by 4 mm thick 1% agarose gel, and electrophoresed at 120−160 V until the BPB (bromophenol blue) tracking dye reached the bottom of the gel. The gel was then dried and autoradiographed. For high-resolution DNA cleavage studies, the cleavage reactions were terminated by precipitation with NaOAc/EtOH, and the precipitate was washed with 70% EtOH and dried. The resulting pellets were resuspended in 5 μL of 80% formamide loading buffer, heat denatured 2 min at 95 °C, loaded onto a 40 cm long by 0.25−0.75 mm thick 1:20 cross-linked 8% polyacrylamide/45% urea gel, and electrophoresed at 1200−2000 V until the BPB tracking dye reached the bottom of the gel. The gel was then dried and autoradiographed.

Densitometry. Optical densitometry was performed using an LKB Bromma Ultroscan XL laser densitometer operating at 633 nm. Sites of significant double-strand cleavage reported in Table 3 were interpolated from the sizes and migration distances of cleavage products relative to those of molecular weight standards. Positions of single-strand cleavage shown in the histograms were obtained by reference to the Maxam−Gilbert G lanes.[30] Relative peak areas for each cleavage band were equated to the relative cleavage efficiencies at those sites and are reflected in the lengths of arrows.

Acknowledgment. This work was supported by Stanford University, the Arnold and Mabel Beckman Foundation, the Camille and Henry Dreyfus Foundation, the Shell Foundation, and an American Cancer Society Institutional Research Grant. D.J.G. was supported by a NSF Predoctoral Fellowship and a Franklin Veatch Fellowship. The UCSF Mass Spectrometry Facility (A. L. Burlingame, Director) is supported by the Biomedical Research Technology Program of the National Center for Research Resources, NIH NCRR BRTP RR04112 and RR01614. We are grateful to Professor Eric Jacobsen (Harvard) for kindly providing a sample of the aldehyde needed to prepare the 5,5-dibromo-3,3′-di-*tert*-butyl derivative **20**.

Supporting Information Available: Spectroscopic and analytical data for metal complexes and procedures for preparation of DNA substrates (16 pages). Ordering information is given on any current masthead page.

IC960196X

(27) (a) Rehmann, J. P.; Barton, J. K. *Biochemistry* **1990**, *29*, 1701−1709. (b) Rehmann, J. P.; Barton, J. K. *Biochemistry* **1990**, *29*, 1710−1717. (c) Eriksson, M.; Leijon, M.; Hiort, C.; Nordén, B.; Gräslund, A. *J. Am. Chem. Soc.* **1992**, *114*, 4933−4934.

(28) (a) Kopka, M. L.; Yoon, C.; Goodsell, D.; Pjura, P.; Dickerson, R. E. *Proc. Natl. Acad. Sci. U.S.A.* **1985**, *82*, 1376. (b) Kopka, M. L.; Yoon, C.; Goodsell, D.; Pjura, P.; Dickerson, R. E. *J. Mol. Biol.* **1985**, *183*, 553−563.

(29) Sambrook, J.; Fritsch, E. F.; Maniatis, T. *Molecular Cloning, A Laboratory Manual*, 2nd ed.; Cold Spring Harbor Laboratory: New York, 1989.

(30) Maxam, A. M.; Gilbert, W. S. *Methods Enzymol.* **1980**, *65*, 499−560.